2015

The Effect Of Direct Electron-positron Pair Production On Relativistic Feedback Rates

Igor B. Vodopiyanov

Joseph R. Dwyer

Eric S. Cramer

R. J. Lucia

Hamid K. Rassoul

AGU PUBLICATIONS

JGR

Journal of Geophysical Research: Space Physics

RESEARCH ARTICLE

10.1002/2014JA020415

Key Points:
- Direct positron creation as contribution to the relativistic feedback mechanism
- Implementation of the direct positron creation process into Monte Carlo
- Positron contribution is significant in compact electric field conditions

Correspondence to:
I. B. Vodopiyanov,
ivodopia@fit.edu

Citation:
Vodopiyanov, I. B., J. R. Dwyer, E. S. Cramer, R. J. Lucia, and H. K. Rassoul (2015), The effect of direct electron-positron pair production on relativistic feedback rates, *J. Geophys. Res. Space Physics*, *120*, 800–806, doi:10.1002/2014JA020415.

Received 25 JUL 2014
Accepted 30 DEC 2014
Accepted article online 7 JAN 2015
Published online 30 JAN 2015

The effect of direct electron-positron pair production on relativistic feedback rates

I. B. Vodopiyanov[1], J. R. Dwyer[1], E. S. Cramer[1], R. J. Lucia[1], and H. K. Rassoul[1]

[1]Department of Physics and Space Sciences, Florida Institute of Technology, Melbourne, Florida, USA

Abstract Runaway electron avalanches developing in thunderclouds in high electric field become self-sustaining due to relativistic feedback via the production of backward propagating positrons and backscattered X-rays. To date, only positrons created from pair production by gamma rays interacting with the air have been considered. In contrast, direct electron-positron pair production, also known as "trident process," occurs from the interaction of energetic runaway electrons with atomic nuclei, and so it does not require the generation of a gamma ray mediator. The positrons produced in this process contribute to relativistic feedback and become especially important when the feedback factor value approaches unity. Then the steady state flux of runaway electrons increases significantly. In certain cases, when the strong electrostatic field forms in a narrow area, the direct positrons become one of processes dominating relativistic feedback. Calculations of the direct positron production contribution to relativistic feedback are presented for different electric field configurations.

1. Introduction

It is now well established that thunderclouds and lightning produce energetic electrons and accompanying X-ray and gamma ray emissions. In high electric field, electrons become runaway if the accelerating force is higher than the drag force due to collision of electrons with air. The electron runaway mechanism, in which electrons may accelerate in static electric fields in air, was first described by *Wilson* [1925]. Then *Gurevich et al.* [1992] showed that when Møller scattering (electron-electron elastic scattering) is included, the runaway electrons described by Wilson will undergo avalanche multiplication, resulting in a large number of relativistic runaway electrons, also see *Gurevich and Zybin* [2001]. This avalanche mechanism is commonly referred to as the Relativistic Runaway Electron Avalanche (RREA) mechanism [*Babich et al.*, 1998, 2001].

Several groups used Monte Carlo codes to simulate processes underlying physics involved in RREA: *Lehtinen et al.* [1999] developed a Monte Carlo that simulated the propagation of energetic electrons in electric and magnetic fields and included energy losses from ionization and atomic excitation, Møller scattering, and angular diffusion from elastic scattering with atomic nuclei. The code did not include bremsstrahlung production. *Babich et al.* [2001, 2004, 2005] used a Monte Carlo called ELIZA, which includes the following elementary processes: for photons, the code includes Compton scattering with allowance for bound electrons, Rayleigh scattering, photo absorption with emission of fluorescent photons and Auger electrons, and production of electron-positron pairs and triplets. For electrons, the code includes elastic scattering by atomic nuclei, ionization and excitation of atomic electron shells, and bremsstrahlung. For positrons, it includes elastic scattering by nuclei, scattering by free electrons, bremsstrahlung, and two body annihilation. *Dwyer* [2003, 2007] developed a Monte Carlo simulation called REAM (runaway electron avalanche model) that included, in an accurate form, all the important interactions involving runaway electrons, including energy losses through ionization and atomic excitation and Møller scattering. Also, this simulation fully models elastic scattering using a shielded Coulomb potential and bremsstrahlung production of X-rays and gamma rays and the subsequent propagation of the photons, including photoelectric absorption, Compton scattering, pair production, and Rayleigh scattering. In addition, the extension to the runaway electron production mechanism, the relativistic feedback discharge (RFD) mechanism is introduced.

In the RFD mechanism, avalanches of runaway electrons emit bremsstrahlung X-rays that may either Compton backscatter or pair produce in air. If the backscattered photons propagate to the start of the avalanche region and produce other runaway electrons either via Compton scattering or photoelectric absorption, then a secondary avalanche develops. Alternatively, the positrons created by gamma to

electron-positron pair conversion often turn around in the ambient electric field and run away in the opposite direction of the electrons. If these positrons propagate to the start of the avalanche region, they can produce additional runaway electrons via hard elastic scattering with atomic electrons in air (Bhahba scattering), thereby producing secondary avalanches. If these positrons annihilate, the annihilation photons could create a seed electron if they propagate to the start of the avalanche region. Also, positrons, accelerated by electric field toward the start of the avalanche region, produce bremsstrahlung which can produce seed electrons as well. If the fractional change in the number of runaway electrons during the feedback cycle, the feedback factor γ, calculated as the ratio of the next generation runaway electron number to the current runaway electron number, is close to or exceeds 1 ($\gamma \sim 1$), the runaway discharge becomes self-sustaining, no longer requiring an external source of energetic seed electrons. For $\gamma > 1$, the number of runaway electron avalanches increases exponentially in time. The feedback factor depends both on electric field strength and length.

The RFD process could explain the intense terrestrial gamma ray flashes (TGF). Modeling and observations performed with spacecraft have shown that a RREA initiated with a cosmic shower cannot create an electron flux intense enough to produce a TGF [*Dwyer*, 2008]. The RFD model introduced by *Dwyer* [2003, 2007] was able to reproduce such characteristics of TGF as electron flux, counts spectrum [*Dwyer and Smith*, 2005], and timing structure of flashes [*Dwyer*, 2012].

Celestin and Pasko [2010] developed a Monte Carlo code that includes the relativistic binary-encounter-Bethe electron impact model to study RREA. This gives slightly different avalanche rates than the Møller scattering. Their Monte Carlo closely followed the work by *Lehtinen et al.* [1999] and, in particular, included an angular diffusion approximation, rather than fully modeling the elastic scattering as in the REAM Monte Carlo code. Their code did not simulate the photons or positrons. The photons, in particular, play an important role in the avalanche development at low fields and so care should be taken when comparing simulations that include bremsstrahlung production and photons propagation (e.g., ELIZA and REAM), especially at very low field values near the avalanche threshold. The recent paper of *Skeltved et al.* [2014] describes the simulation of RREA with RFD using the GEANT4 toolkit. The simulation calculates an avalanche propagation with all the secondary processes and followed by feedback. It shows good agreement with the *Dwyer* [2003, 2007] simulations, including the avalanche parameters, runaway electron spectra, and feedback parameters.

In the RFD model developed by *Dwyer* [2003, 2007], the relativistic feedback mechanisms included are as follows: (1) X-rays Compton backscattered, (2) positrons produced in photon conversion and run away with electric field, (3) positron bremsstrahlung, and (4) positron annihilation.

Among these mechanisms, the positron bremsstrahlung and positron annihilation are the secondary processes with respect to the photon conversion.

Another process to be added is the direct electron-positron pair production via interaction of energetic runaway electrons with atomic nuclei, the "trident process" with three particles in the final state: the scattered projectile electron and an electron-positron pair. Though this process has a low cross section, the positron is produced by electron impact directly, with no intermediate photon involved. Also, both the positron bremsstrahlung and positron annihilation processes get the additional source of positrons from this process.

In this paper, the contribution to the relativistic feedback from the direct electron-positron pair produced by interaction of energetic runaway electrons with atomic nuclei is analyzed for different ambient conditions.

2. Direct Electron-Positron Pair Production

The cross section of the direct production of electron-positron pairs by electrons in the field of a nucleus, in the relativistic limit, is calculated by *Bhabha* [1935]

$$\sigma^{\mathrm{rel}}_{e^- \to e^- e^- e^+} = \frac{28 Z^2 r_e^2 \alpha^2}{27\pi} \ln^3(E_0/mc^2), \tag{1}$$

where Z is the charge of nuclei, r_e is the classical electron radius, α is the fine structure constant, E_0 is the total incident electron energy, and m is the electron mass.

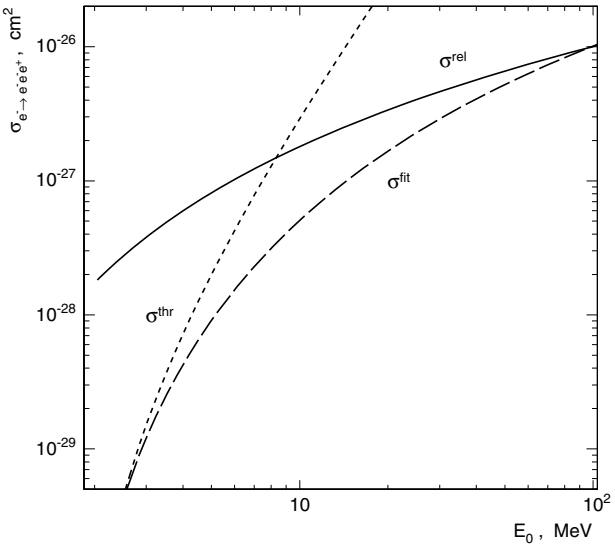

Figure 1. Cross section for the production of electron-positron pairs by relativistic electrons in the field of a nitrogen nuclei as a function of the total incident electron energy. The relativistic approach, cross section near the threshold, and fit over the entire energy range are shown.

The cross section of this process near the threshold is given by *Gryaznykh* [1998]

$$\sigma^{thr}_{e^-\to e^-e^-e^+} = \frac{7Z^2 r_e^2 \alpha^2}{2304} \frac{(T_0 - 2mc^2)^3}{(mc^2)^3}, \quad (2)$$

where T_0 is the incident electron kinetic energy.

A fit to the numerical results over the entire energy range is taken from [*Gryaznykh*, 1998]

$$\sigma^{fit}_{e^-\to e^-e^-e^+} = 5.22Z^2 \ln^3\left(\frac{2.3+T_0\,[\mathrm{MeV}]}{3.52}\right) \mu\mathrm{b}. \quad (3)$$

This fit function, in the E_0 range of interest, 3 MeV to 100 MeV, is used further as the cross section in the Monte Carlo code, with the average air Z and air nuclear density values. Figure 1 shows the cross section for a nitrogen nucleus as function of the total incident electron energy.

The total energy of the created electron-positron pair, E_e+E_p, is a fraction of the incident electron energy E_0. To obtain the E_e+E_p distribution, the formulas for the relativistic and low-energy approaches derived by *Bhabha* [1935] and interpolation between low- and high-energy subranges are used. Figure 2 presents several distributions calculated for different incident electron energies as a function of E_e+E_p.

3. Monte Carlo Simulation

In this paper, the relativistic runaway electron avalanche model (REAM) Monte Carlo code [*Dwyer*, 2003, 2007], modeling the RFD, is used. It is capable of simulating the development and propagation of runaway electron avalanches in a gaseous medium with magnetic and electric fields. The simulation includes all the important interactions of electrons, positrons, and gamma rays. These interactions include energy losses due to ionization and atomic excitation, and elastic scattering of electrons on electrons (Møller scattering) and on nuclei (Coulomb scattering). Production of X-rays is modeled including bremsstrahlung and positron annihilation; the subsequent propagation of X-rays includes photoelectric absorption, Rayleigh scattering, Compton scattering, and pair production. Also, the simulation includes positron propagation and generation of energetic seed electrons via Bhabha scattering of positrons as well as via Compton scattering and photoelectric absorption of energetic photons.

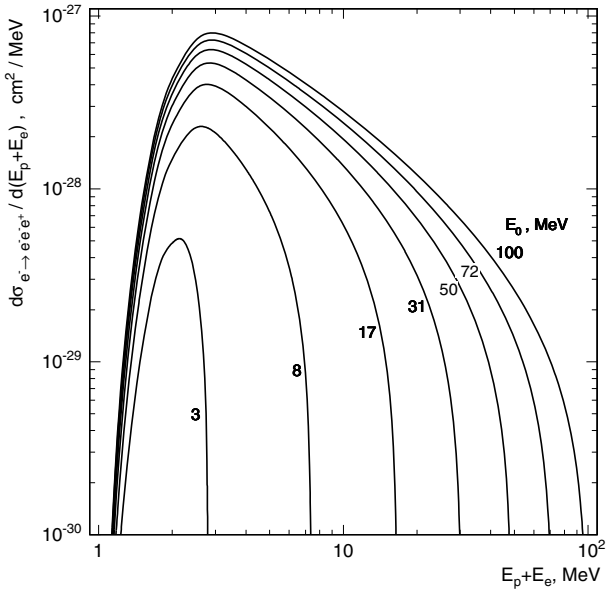

Figure 2. Differential cross section for the direct production of the electron-positron pair as a function of the total electron-positron pair energy, E_e+E_p, for different incident electron energies.

The REAM code is extended with the process of the direct electron-positron pair production via interaction of energetic electrons with atomic nuclei. Such an

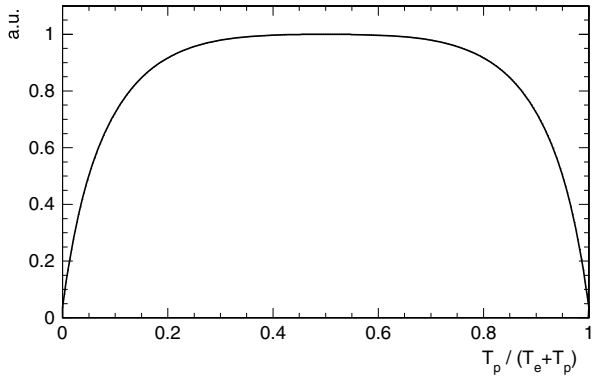

Figure 3. Relative kinetic energy distribution of a positron created in the direct electron-positron pair production, used in Monte Carlo.

interaction is simulated for electrons with energy above 3 MeV using the cross section represented with equation (3) and Figure 1. Total energy of the created electron-positron pair E_e+E_p is simulated according to the differential cross section $d\sigma_{e^-\to e^-e^-e^+}/d(E_e+E_p)$, taken from the formula (30) of *Bhabha* [1935] for the low-energy limit, formula (34) of *Bhabha* [1935] for the relativistic case, and interpolation function for intermediate energies; corresponding distributions are presented in Figure 2. This sum energy is randomly distributed between electron and positron. To simulate the positron energy, two approximations are used.

First, in the approach $E_e \gg mc^2$, $E_p \gg mc^2$ and $E_0 \gg E_e$, $E_0 \gg E_p$, such a distribution is determined by the term from the double differential cross section, formula (32) of *Bhabha* [1935]:

$$\frac{E_e^2+E_p^2+\frac{2}{3}E_eE_p}{(E_e+E_p)^4}\ln\frac{E_eE_p}{(E_e+E_p)mc^2}\ln\frac{E_0}{E_e+E_p}. \tag{4}$$

From that, one can find that the relative positron kinetic energy $T_p/(T_e+T_p)$ distribution is symmetric with respect to the condition $T_p=T_e$ and suppressed at $T_p\sim0$ and $T_e\sim0$; in the simulation, the generic shape shown in Figure 3 is used for all the energies of the incident electrons above 3 MeV. It is worth to note that the low-energy case, when this approximation is not valid, is much less important for positron feedback, because low-energy positron has much high probability to annihilate.

Second, the positron direction is always chosen to be the same as the direction of the incident electron. This approach is considered to be conservative, preventing overestimation of feedback, because incident electrons, such as the runaway ones, move generally toward the direction of electric field; however, a positron, to contribute to feedback, should be turned back by this field and accelerate to the runaway energy. Thus, this approximation dilutes further the uncertainty which may be introduced by the first approximation when the electron-positron pair has low energy.

These positrons are then involved in all the consequent steps of simulation, including the bremsstrahlung and annihilation processes.

The incident electron direction is assumed to be unchanged. This is considered to be good approach because in direct pair creation, on average, electron loses a small part of its energy. The electron created in such an act of pair production is not considered further, because the contribution of a single electron to a developed avalanche is negligible; in other words, the Møller scattering, responsible for the multiplication of runaway electrons in an avalanche, has cross section much greater than the direct pair production cross section.

4. Results

To estimate contributions of different mechanisms to the relativistic feedback, the simulations are run up to completion of two generations of electron avalanches. The first generation avalanche is started with a seed electron injected at a start point, where electrons are accelerated by the electric field. While an avalanche develops, the runaway electrons create secondary particles, some of them propagate backward and create other seed electrons; then the second generation avalanche can start developing. Simulation is stopped when all the particles of two generations are tracked until they either lose energy or escape the simulation region. The feedback factor γ is determined as the ratio of the number of runaway electrons in the second avalanche(s) to the first avalanche(s), where electrons are counted when passing the plane midway between the top and bottom of the avalanche region.

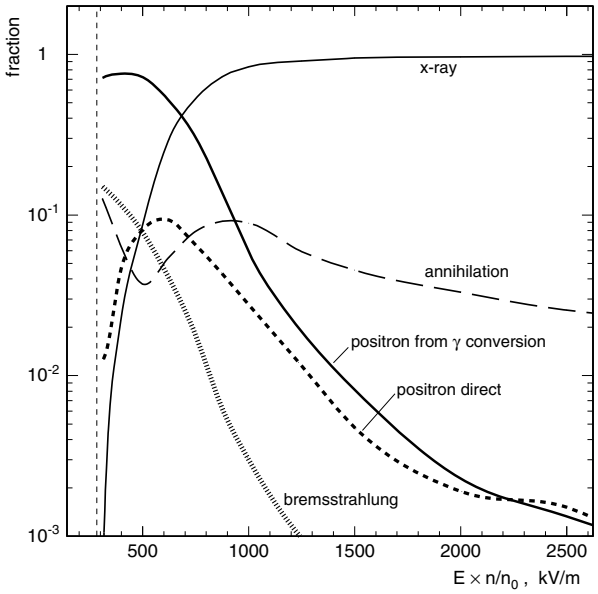

Figure 4. Relative contributions to the total feedback from X-ray, positron from gamma conversion, positron from direct pair production, positron bremsstrahlung, and positron annihilation feedback for air as a function of the uniform electric field strength. The factor n/n_0 scales the electric field E, from the sea level air density to the ambient one. The vertical dashed line shows the value of the runaway avalanche threshold field, E_{th}.

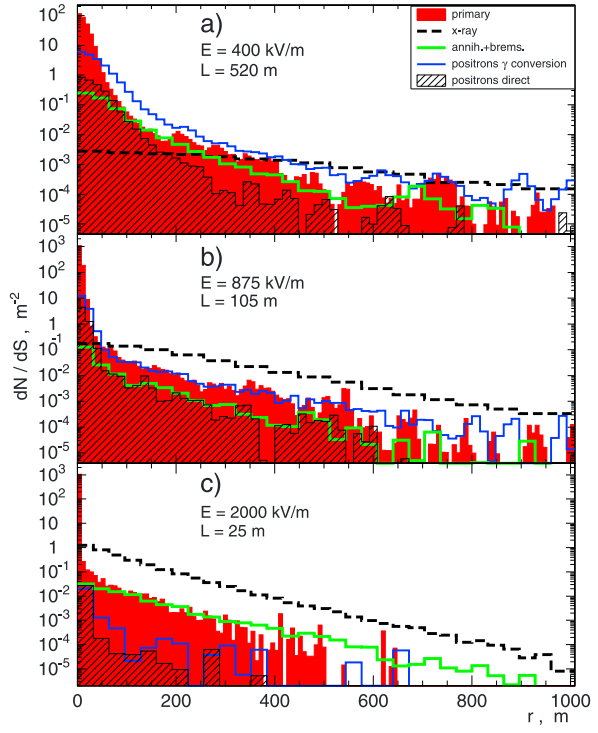

Figure 5. Profiles of electron avalanches at the midway of the uniform wide electric field region. dN/dS represents the number of electrons crossing the ring with area dS at distance r from the primary avalanche axis. Primary avalanches and secondary avalanches resulting from different feedback processes developed in electric field E of length L are shown.

The feedback factor depends on the electric field strength and the electric field length. The simulation region is always greater than the electric field region, so that contributions of all the particles created, including the secondaries, are taken into account. To estimate the feedback contributions at conditions under which electron avalanches become self-sustaining, the electric field parameters are selected so that $\gamma \sim 1$.

First, the simulation is performed using the uniform cylindrical shape electric field, where the cylinder radius is much greater than the cylinder length, $R \gg L$, and E is parallel to the cylinder axis. Figure 4 presents the results of simulations, as partial contributions of each process to the total feedback, where sum of all contributions is normalized to unit, performed at a set of electric field strengths. The results for the four previously identified feedback processes agree with [*Dwyer*, 2007].

As can be seen, the positron contribution dominates at low field strengths, and the X-ray contribution dominates at high field strengths. This is because keeping the feedback factor close to 1 results in setting the field region length L to a certain value for each electric field strength, so that for the uniform field, it changes from 1500 m at 325 kV/m to 19 m at 2500 kV/m. For the positron feedbacks, the direct positron contribution is generally less significant than the gamma conversion positron contribution; they become comparable only at high field.

Figure 5 presents the different feedback contributions to the electron avalanches as the profiles of the corresponding avalanches at the midplane $(L/2)$, for different electric field strengths. Profiles are determined as the number of electrons passed the midplane as a function of the transverse coordinate (radial distance r).

The profile parameters are listed in Table 1.

The primary and secondary avalanches caused by positrons have relatively small lateral spreads. The higher the electric field strength the smaller the spread, because the runaway electrons and positrons are forced by the electric field to move parallel to its direction. The gamma conversion positron profiles are a little wider than the

Table 1. Parameters of the Secondary Avalanches: Average Partial Yields of the Processes and Spreads of the Avalanche Profiles as Standard Deviations σ [a]

	Positron γ Conversion		Positron Direct		X-ray	
E (kV/m)	Yield (%)	σ (m)	Yield (%)	σ (m)	Yield (%)	σ (m)
400	70	37	8.7	30	9.7	256
875	15	27	4.5	17	79	136
2000	0.23	36	0.19	16	96	77
Nonuniform	40	21	20	21	35	25

[a]First three rows correspond to the cases from Figure 5. Last row corresponds to the special case, Figure 6, described further in this paper.

direct positron ones, because their creation is mediated with the photons, introducing additional spread. The Compton backscattered X-rays are not affected by the electric force; therefore, the avalanches caused by them have much larger spreads.

If one shrinks the electric field region, decreasing R at the same L, the relative contribution to feedback from X-rays decreases with respect to the positrons, and the feedback from the direct positrons increases with respect to the gamma conversion positrons. A simulation with a narrower field configuration, as drawn in Figure 6 (top), was performed. This field is generated with the negative charge sphere of radius 25 m with the electric field strength 2000 kV/m on its surface, and the positive charge sphere of radius 45 m with the electric field strength 1400 kV/m on its surface located 190 m apart from the first sphere. For such a condition, the feedback factor is close to 1. Figure 6, bottom, presents the resulting avalanche profiles.

The profile parameters are listed in Table 1, last row.

In such a field configuration, the second-generation avalanche can develop only in the vicinity of the first sphere or within a limited radius around the line between spheres, where the electric field strength is high enough. Therefore, despite the fact that the strength of this field is comparable to that of Figure 5b, the contribution to the feedback from the scattered X-rays is only 35%, and the contributions from the gamma conversion positrons and from the direct positrons are 40% and 20%, respectively.

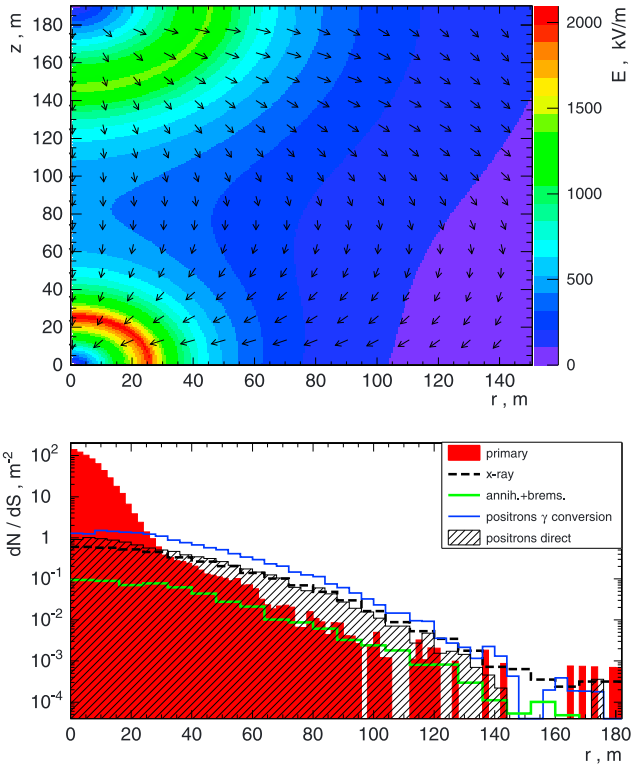

Figure 6. (top) Electric field strength map. The color-coded strength value is plotted in coordinates of the distance between the charged sphere centers, z, versus the radial distance r. The electric field direction is shown with arrows. (bottom) Profiles of electron avalanches at the midway of the electric field region, plotted on the top. dN/dS represents the number of electrons crossing the ring with area dS at distance r. Primary avalanches, and secondary avalanches resulting from different feedback processes, are shown.

5. Conclusion

In this paper, we analyze the process of direct electron-positron pair production via the interaction of energetic runaway electrons with atomic nuclei as the additional process contributing to the RFD. A set of tests is performed using the REAM Monte Carlo software.

The simulations shows that different secondary processes occurring in electron avalanche development can create significant feedback resulting in development of secondary electron avalanches, depending upon the configurations and strengths of the electric field.

As the direct positrons are produced by runaway electrons with no photon mediators, their initial distribution in the transverse direction with respect to the axis of the primary avalanche plane is essentially the same as that of

the runaway electrons of the primary avalanche. Therefore, when these positrons are eventually turned around by the electric field and become the runaway, the secondary electron avalanches are initiated with them predominantly close to the primary avalanche axis. Secondary electron avalanches created with any other mechanism contributing to the relativistic feedback have a larger spatial spread. Therefore, the direct positron production significantly contributes to feedback especially in cases of a narrow electric field.

Acknowledgments

This work was supported by DARPA HR0011-1-10-1-0061 and NASA GSRP NNX09AJ16H. Requests for data used to generate or be displayed in figures, graphs, plots, or tables may be made to the corresponding author.

Michael Balikhin thanks the reviewers for their assistance in evaluating this paper.

References

Babich, L. P., I. Kutsyk, E. Donskoy, and A. Kudryavtsev (1998), New data on space and time scales of relativistic runaway electron avalanche for thunderstorm environment: Monte Carlo calculations, *Phys. Lett. A*, *245*(5), 460–470.

Babich, L. P., E. N. Donskoy, I. M. Kutsyk, A. Y. Kudryavtsev, R. A. Roussel-Dupré, B. N. Shamraev, and E. M. Symbalisty (2001), Comparison of relativistic runaway electron avalanche rates obtained from Monte Carlo simulations and kinetic equation solution, *IEEE Trans. Plasma Sci.*, *29*(3), 430–438.

Babich, L. P., E. N. Donskoy, R. I. Ilkaev, I. M. Kutsyk, and R. A. Roussel-Dupré (2004), Fundamental parameters of a relativistic runaway electron avalanche in air, *Plasma Phys. Rep.*, *30*(7), 616–624.

Babich, L. P., E. N. Donskoy, and I. M. Kutsyk (2005), The feedback mechanism of runaway air breakdown, *Geophys. Res. Lett.*, *32*, L9809, doi:10.1029/2004GL021744.

Bhabha, H. J. (1935), The creation of electron pairs by fast charged particles, *Proc. R. Soc. London, Ser. A*, *152*, 559–586, doi:10.1098/rspa.1935.0208.

Celestin, S., and V. P. Pasko (2010), Soft collisions in relativistic runaway electron avalanches, *J. Phys. D: Appl. Phys.*, *43*, 315206, doi:10.1088/0022-3727/43/31/315206.

Dwyer, J. (2003), A fundamental limit on electric fields in air, *Geophys. Res. Lett.*, *30*(20), 2055, doi:10.1029/2003GL017781.

Dwyer, J. (2007), Relativistic breakdown in planetary atmospheres, *Phys. Plasmas*, *14*, 42901, doi:10.1063/1.2709652.

Dwyer, J. (2008), Source mechanisms of terrestrial gamma-ray flashes, *J. Geophys. Res.*, *113*, D10103, doi:10.1029/2007JD009248.

Dwyer, J. (2012), The relativistic feedback discharge model of terrestrial gamma ray flashes, *J. Geophys. Res.*, *117*(A2), A02308, doi:10.1029/2011JA017160.

Dwyer, J., and D. Smith (2005), A comparison between Monte Carlo simulations of runaway breakdown and terrestrial gamma-ray flash observations, *Geophys. Res. Lett.*, *32*, L22804, doi:10.1029/2005GL023848.

Gryaznykh, D. A. (1998), Cross section for the production of electron-positron pairs by electrons in the field of a nucleus, *Phys. At. Nucl.*, *61*(3), 394–399.

Gurevich, A., and K. Zybin (2001), Runaway breakdown and electric discharges in thunderstorms, *Phys. Usp.*, *44*(11), 1119–1140, doi:10.1070/PU2001v044n11ABEH000939.

Gurevich, A., G. Milikh, and R. Roussel-Dupré (1992), Runaway electron mechanism of air breakdown and preconditioning during a thunderstorm, *Phys. Lett. A*, *165*(5–6), 463–468.

Lehtinen, N., T. Bell, and U. Inan (1999), Monte Carlo simulation of runaway MeV electron breakdown with application to red sprites and terrestrial gamma ray flashes, *J. Geophys. Res.*, *104*(24), 699–24.

Skeltved, A. B., N. Østgaard, B. Carlson, T. Gjesteland, and S. Celestin (2014), Modeling the relativistic runaway electron avalanche and the feedback mechanism with GEANT4, *J. Geophys. Res. Space Physics*, *119*, 9174–9191, doi:10.1002/2014JA020504.

Wilson, C. (1925), The acceleration of β-particles in strong electric fields such as those of thunderclouds, *Math. Proc. Cambridge Philos. Soc.*, *22*(04), 534–538, doi:10.1017/S0305004100003236.